FEBS 28558 FEBS Letters 570 (2004) 13–19

Structures of *Bacillus subtilis* PdaA, a family 4 carbohydrate esterase, and a complex with *N*-acetyl-glucosamine

David E. Blair, Daan M.F. van Aalten*

Division of Biological Chemistry and Molecular Microbiology, School of Life Sciences, University of Dundee, Dundee DD1 5EH, UK

Received 5 May 2004; revised 4 June 2004; accepted 5 June 2004

Available online 15 June 2004

Edited by Hans Eklund

Abstract Family 4 carbohydrate esterases deacetylate polymeric carbohydrate substrates such as chitin, acetyl xylan and peptidoglycan. Although some of these enzymes have recently been enzymologically characterised, neither their structure nor their reaction mechanism has been defined. Sequence conservation in this family has pointed to a conserved core, termed the NodB homology domain. We describe the cloning, purification and 1.9 Å crystal structure of PdaA, a peptidoglycan deacetylase from *Bacillus subtilis*. The enzyme assumes a fold related to a $(\beta/\alpha)_8$ barrel, with a long groove on the surface of the protein that harbours all conserved residues. A complex with the substrate analogue *N*-acetyl-glucosamine was refined to 2.25 Å resolution, revealing interactions of an aspartic acid and three histidines, all conserved in the NodB homology domain, with the ligand. The PdaA structure provides a template for interpreting the wealth of sequence data on family 4 carbohydrate esterases in a structural context and represents a first step towards understanding the reaction mechanism of this family of enzymes.

Keywords: Family 4 carbohydrate esterase; PdaA; *N*-Acetyl-glucosamine; *Bacillus subtilis*

1. Introduction

Family 4 carbohydrate esterases (CE-4, CAZY classification, http://afmb.cnrs-mrs.fr/CAZY) deacetylate a wide variety of acetylated poly/oligosaccharides [1] (Fig. 1A). Chitin deacetylases (partially) deacetylate chitin (a polymer of β (1,4)-linked *N*-acetyl glucosamine) to chitosan, a component of the fungal cell wall/spore cortex [2–4]. NodB is a rhizobial protein that deacetylates Nod-factors, chitinous lipooligosaccharides that regulate the symbiotic relationships between leguminous plants and nitrogen fixing bacteria [5,6]. Acetyl xylan esterases deacetylate *O*-acetylated xylan, a key component of plant cell walls [1]. Peptidoglycan deacetylases de-*N*-acetylate the *N*-acetyl-muramic acid and *N*-acetyl-glucosamine residues of the di-sugar repeats in bacterial peptidoglycan [7,8]. Through sequence alignments of CE-4 esterases it has become apparent that these enzymes contain a conserved catalytic core, termed the NodB homology domain [1,2]. Although many CE-4 enzymes have been cloned and characterised in terms of their substrate preferences and kinetics (e.g. [1,4,6,8–11]), it is not known which of the residues conserved in the NodB homology domain are required for substrate binding/specificity and catalytic activity, and no CE-4 structure has so far been reported.

PdaA is a *Bacillus subtilis* CE-4 esterase, acting on peptidoglycan [8,12]. Up to half of the *N*-acetyl-muramic acid residues in *B. subtilis* spore cortex peptidoglycan are deacetylated and lactamised to muramic δ-lactam [13] (Fig. 1A). These δ-lactam residues are required for germination lytic enzymes [14]. PdaA acts together with CwlD, a muramoyl L-alanine amidase which hydrolyses the muramic acid–peptide linkages [8,12,14]. Expression of PdaA and CwlD together in *Escherichia coli* is sufficient for formation of muramic δ-lactam residues in *E. coli* peptidoglycan [12]. The PdaA amino acid sequence aligns well with NodB homology domains of representative CE-4 esterases (Fig. 1B) and could therefore serve as a template for interpretation of the structure and mechanism of this family of enzymes. As a first step towards this goal, we describe the crystal structure of PdaA and complexes with *N*-acetyl glucosamine and cadmium. These structures define the geometry of the CE-4 esterase active site, demonstrating that the conserved residues of the NodB homology domain line a substrate binding groove.

2. Materials and methods

2.1. Cloning, purification and crystallisation

A fragment corresponding to PdaA was amplified by PCR using the Expand High Fidelity PCR system (Roche), with *B. subtilis genomic* DNA as the template (forward primer: 5′ GATCCGTATTG CTTGCCGGAGGTGCACAG 3′, reverse primer: 5′ GGATCCTT ACAAAGACGGCAGCCTCATTC 3′). The amplified DNA fragment encoded the entire length of the *pdaa* gene with the exception of the proposed N-terminal signal sequence (MKWMCSICCAA). The resulting PCR product was ligated into pCR 2.1-TOPO (Invitrogen) and sub cloned into the pGEX-6P-1 vector. The construct sequence was verified by DNA sequencing (The Sequencing Service, School of Life Sciences, University of Dundee, Scotland, UK).

The PdaA-pGEX-6P-1 construct was transformed into *E. coli* BL21-DE3 pLysS cells. Cells were grown overnight in Luria–Bertani medium (LB) + ampicillin (100 μg/ml). From this culture 10 ml of cells was used to further inoculate 1 litre of LB media. The cells were grown to $OD_{600} = 0.6$ at 37 °C before protein expression was induced by the addition of 100 μM of isopropyl-β-D-thiogalactopyranoside and then the cells were cultured for an additional 18 h at room temperature. The cells were harvested by centrifugation at 2250×*g* for 30 min and the cell pellet from each litre of culture was resuspended in 40 ml of LB media and subjected to centrifugation as previous. The resulting cell pellets were flash frozen in liquid nitrogen, thawed at 37 °C in a water bath and resuspended in 25 ml of lysis buffer (25 mM Tris–HCl, 2 mM EDTA, 250 mM NaCl, 5 mM DTT, pH 7.5, and 0.5 tablet of 'Complete' protease inhibitor cocktail tablets (Roche)). Lysis was achieved

* Corresponding author. Fax: +44-1382-345764.
E-mail address: dava@davapc1.bioch.dundee.ac.uk (D.M.F. van Aalten).

0014-5793/$22.00
doi:10.1016/j.febslet.2004.06.013

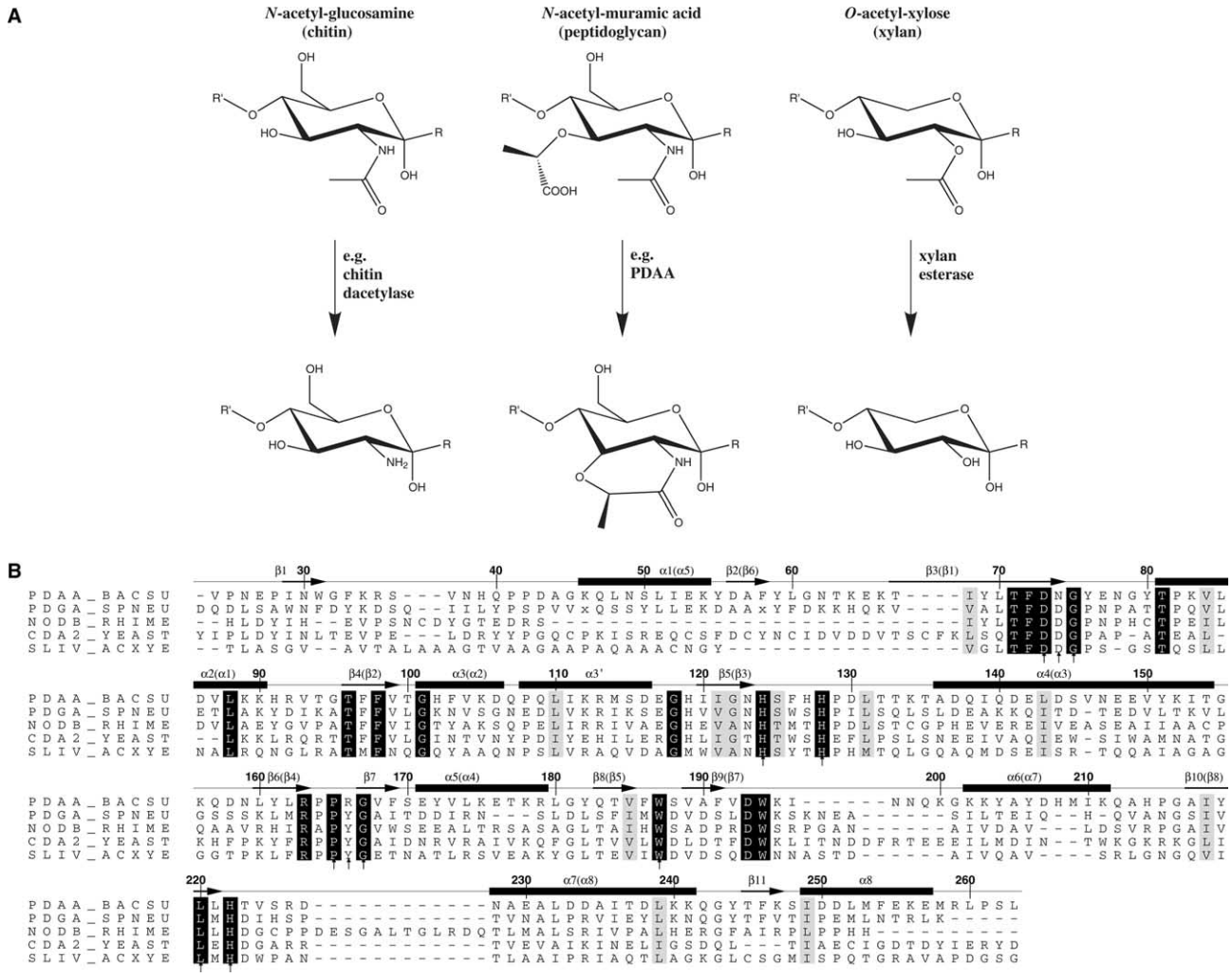

Fig. 1. Activity and sequence conservation of family 4 carbohydrate esterases. (A) Substrates recognised and reactions performed by family CE-4 esterases. (B) Sequence alignment of four diverse representatives of the CE-4 family. PDAA_BACSU = *Bacillus subtilis* polysaccharide deacetylase, PDGA_SPNEU = *Streptococcus pneumoniae* peptidoglycan deacetylase, NODB_RHIME = *Rhizobium meliloti* nodulation protein B, CDA2_YEAST = *Saccharomyces cerevisiae* chitin deacetylase 2, SLIV_ACXYE = *Streptomyces lividans* acetyl xylan esterase. Sequence numbers following PdaA numbering. Fully conserved residues are shaded black, partially conserved residues are shaded grey. PdaA secondary structure elements are shown and labelled, the labels between brackets refer to secondary structure nomenclature in the canonical $(\beta/\alpha)_8$ fold. Arrows indicate residues that interact with *N*-acetyl-glucosamine in the PdaA–GlcNAc complex.

by the addition of 10 mg DNAse-1 and 0.5 mg/ml lysozyme incubating for 20 min on ice and finally, 5×30 s cycles of sonication. The lysate was centrifuged at $40\,000 \times g$ for 30 min to remove residual debris before passing the supernatant through a 0.45 μm filter. The supernatant was then incubated at 4 °C on a rotating platform with glutathione–Sepharose pre-washed with lysis buffer in a ratio of 3 ml of beads per litre of bacterial culture for 2 h. The N-terminal GST tag was removed from the GST-PdaA fusion protein by incubating the beads with PreScission protease (50 μg protease per ml of beads) at 4 °C for 18 h. The supernatant of the beads and a subsequent wash were passed over a BioRad 20 ml disposable column to remove the beads. The resulting filtrate was then concentrated to 4 ml and loaded onto a Superdex 75, 26/60 gel filtration column equilibrated in buffer (25 mM Tris–HCl, 150 mM NaCl, 2 mM EDTA, pH 7.5). The pure fractions were verified by SDS–PAGE.

PdaA was concentrated to 22 mg/ml with a VivaScience concentrator (10 000 MW cut off) as verified by a Bradford assay. The sitting drop vapour diffusion method was used to produce crystals by mixing 1 μl of protein solution with 1 μl of a mother liquor solution (20% (w/v) PEG 12000, 0.1 M HEPES, pH 7.5). Crystal growth improved by the addition 10 μl of 100 mM $CdCl_2$ to 100 μl of mother liquor. Hexagonal crystals grew within 4 days. Crystals were frozen in a nitrogen gas stream cooled to 100 K after being cryo-protected transiently in mother liquor containing 10% glycerol. Soaks with *N*-acetyl-glucosamine were carried out by removing a crystal from the crystallisation drop and soaking in mother liquor containing 1 M *N*-acetyl-glucosamine for 3 h prior to freezing. All the heavy atom soaks were achieved by addition of 0.5 μl of 100 mM heavy atoms solutions/suspensions to the crystal drops.

2.2. Data collection, structure solution and refinement

Data were collected on PdaA, PdaA_GlcNAc and Cd/Pt derivatives as shown in Table 1. Using the native data set as a reference, the two Cd derivatives and the Pt derivative were used for multiple isomorphous replacement with anomalous scattering (MIRAS) phasing with MLPHARE [15], giving phases to 3.5 Å with a figure of merit of 0.54. From Matthews coefficient calculations two monomers per asymmetric unit were predicted ($V_M = 2.3$ Å^3/Da, solvent content = 47%). A pseudo twofold rotation axis was located from the refined heavy atom sites with FINDNCS [16] and used for averaging together with solvent flattening and phase extension with DM [17] and RESOLVE [18]. A map calculated with the resulting phases to 1.9 Å revealed well defined protein-like electron density. WarpNtrace [19] was then used to automatically interpret this map, building 419 out of 514 residues in the

Table 1
Details of data collection and structure refinement

Data set	Native	GlcNAc	$CdCl_2$a	$CdCl_2$b	$PtCl_4$
X-ray source	DESY-X11	ESRF-BM14	home	DESY-X11	DESY-X11
Wavelength (Å)	0.8123	1.0085	1.5418	0.8123	0.8123
Resolution range (Å)	15.00–1.90 (1.97–1.90)	20.00–2.25 (2.33–2.25)	25.00–2.10 (2.18–2.10)	15.00–2.50 (2.59–2.50)	15.00–3.00 (3.11–3.00)
# Observed reflections	159 789 (16 031)	73 498 (5185)	186 640 (17 852)	65 964 (6607)	63 658 (6975)
# Unique reflections	41 729 (4171)	24 612 (2182)	30 220 (3040)	18 577 (1854)	9991 (1055)
Redundancy	3.8 (3.8)	3.0 (2.4)	6.2 (5.9)	3.6 (3.6)	6.4 (6.6)
$I/\sigma I$	10.9 (3.8)	10.5 (1.8)	8.5 (2.6)	7.3 (2.4)	9.5 (3.1)
Completeness (%)	99.9 (100.0)	98.6 (98.2)	98.5 (97.8)	99.9 (100.0)	100.0 (100.0)
R_{merge}	0.069 (0.449)	0.107 (0.556)	0.107 (0.648)	0.129 (0.553)	0.103 (0.619)
Number of sites			4	6	6
Phasing power cen/acen	–	–	1.55/1.27	0.74/0.55	0.95/0.72
R_{cryst}, R_{free}	0.201/0.261	0.202/0.258	0.179/0.227		
Groups/$\langle B \rangle$ (Å^2)					
Amino acids	469/25.6	470/37.4	469/29.0		
Water	366/29.9	258/36.3	325/31.4		
Ligand	–	2 GlcNAc/50.9	4 Cd^{2+}/29.3		
RMSD from ideal geometry					
Bonds (Å)	0.010	0.008	0.10		
Angles (°C)	1.5	1.3	1.4		
B-factor RMSD (Å^2) (bonded, main chain)	1.4	1.4	1.4		

Values between brackets are for the highest resolution shell. Crystals were of space group $P6_5$ and were cryo-cooled to 100 K. All measured data were included in structure refinement.

asymmetric unit. This model was then used as a starting point for further building in O [20], interspersed with refinement using CNS [21] (Table 1). Refinement of the complexes with cadmium and *N*-acetylglucosamine was started from the final native structure, following a similar procedure (Table 1). Models for the ligands were not included until fully defined by unbiased $|F_o| - |F_c|$, ϕ_{calc} maps. The conformation of the two molecules in the asymmetric unit is virtually identical (all-atom RMSD = 0.24 Å for the monomers in the native structure) and the "A" monomer was used consistently for structural analyses and comparisons. Pictures were made with PyMol (http://www.pymol.org).

3. Results and discussion

3.1. Overall structure

PdaA was cloned from *B. subtilis* genomic DNA and overexpressed as a fusion protein in *E. coli*, yielding 5 mg of final purified protein per litre of bacterial culture. The protein was crystallised from PEG solutions, synchrotron diffraction data were collected and the structure was solved by MIRAS (Table 1). The native structure was refined to 1.9 Å resolution with $R = 0.201$ ($R_{free} = 0.261$) (Table 1). The structure reveals a modified $(\beta/\alpha))_8$ fold (Fig. 2A). Query of the PDB database identified an entry of a selenomethionine labeled PdaA (entry 1NY1), although no report on this structure has been published. Our native PdaA structure superimposes on PDB entry 1NY1 with an RMSD of 0.3 Å and the structure reported here will be used for further analyses and discussion. Searches for structural similarity with DALI [22] identified several $(\beta/\alpha)_8$ proteins, including Tiny-TIM ([23], Fig. 2A), which contains a minimal $(\beta/\alpha)_8$ fold (RMSD = 3.2 Å on 131 C_α atoms). However, there are a few notable differences from the canonical $(\beta/\alpha)_8$ fold. First, PdaA contains an extra *N*-terminal β-strand (β 1, Figs. 1B and 2A) which pairs with a further additional β-strand (β7) to form a small β-sheet. An extra β-strand (β11) and α-helix (α8) at the C-terminus seal the bottom of the barrel. Strikingly, the PdaA *N*-terminal helix α1 occupies a topological position equivalent to helix α5 in the canonical $(\beta/\alpha)_8$ fold (Figs. 1B and 2A). Similarly, PdaA strand β2 lies in place of β6 in the standard $(\beta/\alpha)_8$ fold. To our knowledge, this type of "secondary structure swapping" has not been previously observed in $(\beta/\alpha)_8$ folds and searches with DALI did not reveal similar topological arrangements.

3.2. The active site

In the PdaA structure, the residues conserved in the NodB homology domain are clustered in a groove on the face of the protein (Figs. 2B and 3). This groove is approximately 30 Å long and 9 Å wide. The N-terminus, which is variable in length across the CE-4 family (Fig. 1B), forms one end of this groove (Fig. 2B). The section of the groove covering the conserved residues has acidic surface charge characteristics, whereas the end of the groove corresponding to the PdaA N-terminus is positively charged. Compared to the other CE-4 esterases, PdaA possesses three additional basic residues that line the groove, Lys34, Arg35 and Arg166. These positive charges could serve a role in recognition of and interaction with the *O*-lactoyl groups on the peptidoglycan muramic acid residues, which are not present in the other substrates (e.g. chitin, acetyl xylan) recognised by family CE-4 esterases. The observed groove is compatible with the fact that members of the CE-4 family all recognise multimeric substrates. This has been particularly well studied for the chitin deacetylases, which need at least a $(GlcNAc)_3$ trimer for activity, but prefer longer chitooligosaccharides [4,9,11,24]. The conserved residues in the groove observed in the PdaA structure would create space for at least three subsites, which are thus likely to be present in all proteins containing the NodB homology domain.

The deepest section of the groove contains a number of unusual features. The conserved Asp73 lies at the bottom of

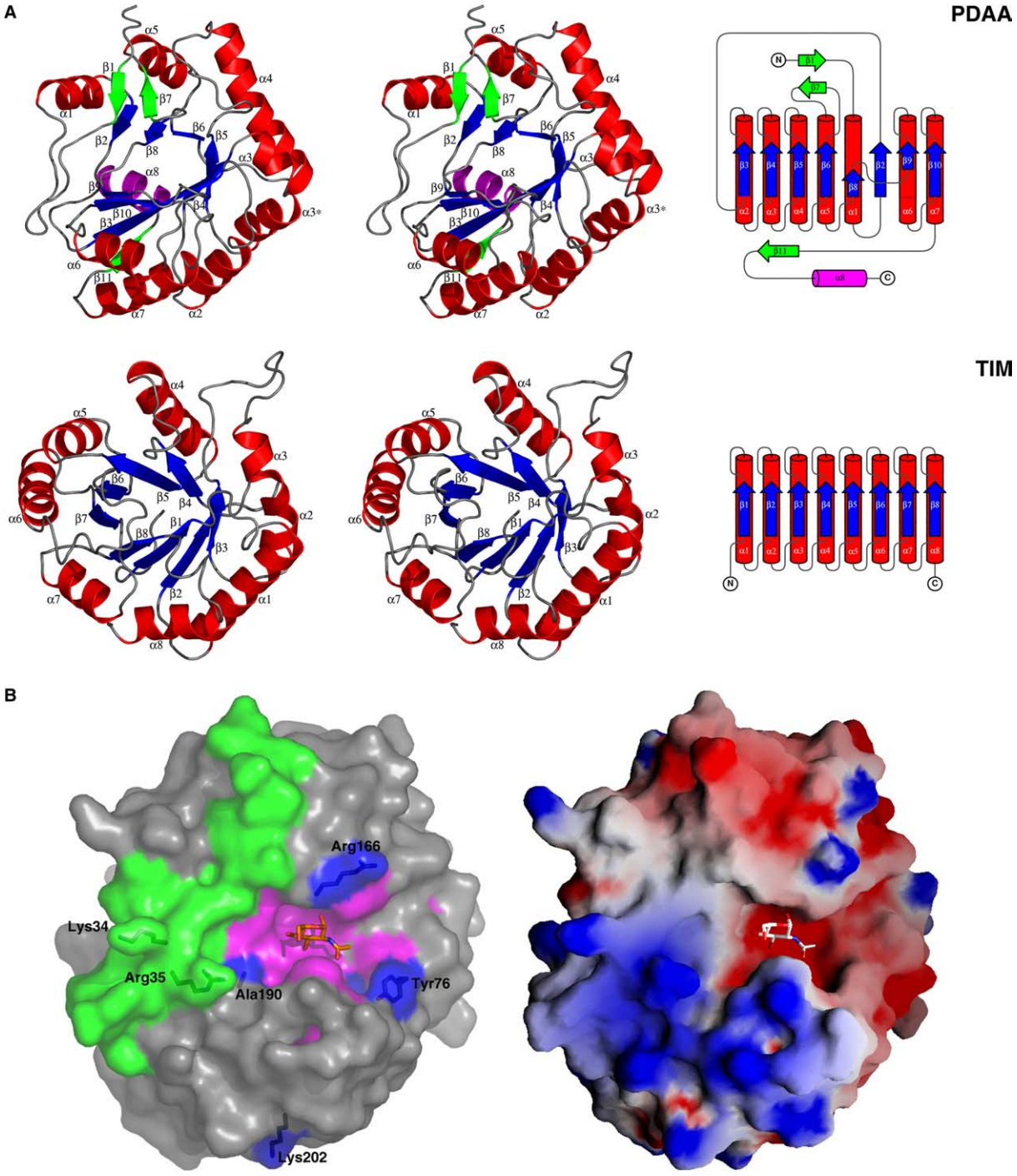

Fig. 2. PdaA structure, topology and surface properties. (A) Stereo images of PdaA and the canonical TIM barrel $(\beta/\alpha)_8$ fold as observed in Tiny-TIM [23], alongside their topological representations as generated with TopDraw [32]. PdaA secondary structure elements without equivalents in the TIM barrel fold are coloured green (strands) or magenta (helix). (B) Left: sequence conservation as seen in Fig. 1B. Residues not conserved in the CE-4 family are coloured grey. Residues conserved in all CE-4 members shown in Fig. 1B are coloured magenta. Residues conserved in all CE-4 members, apart from PdaA, are coloured blue. The poorly conserved *N*-terminus of PdaA is coloured green. Right: surface electrostatics calculated with GRASP [33], from red (−5 kT) to blue (+5 kT). In addition to the surfaces, the GlcNAc observed in the PdaA–GlcNAc data set is shown in a sticks representation.

this groove. Interestingly, behind Asp73, deeper into the core of the enzyme, lies a conserved arginine (Arg163) which is buried into a hydrophobic pocket, formed by the conserved residues Phe98, Trp187 and Leu220 (Fig. 3). Similarly, His222 lies on the side of the groove, and behind it lies Asp193, buried in a hydrophobic pocket (Fig. 3). The buried Arg163 and Asp193 could serve to stabilise charges on Asp73 and His222 during the reaction, or tune the pK_a of these residues. The coordinates of these Asp73–Arg63 and His222–Asp193 charge–relay pairs were used in a search for similar active sites in known protein structures using the SPASM database [25], yet no hits were found. Similar searches with Asp73, His222

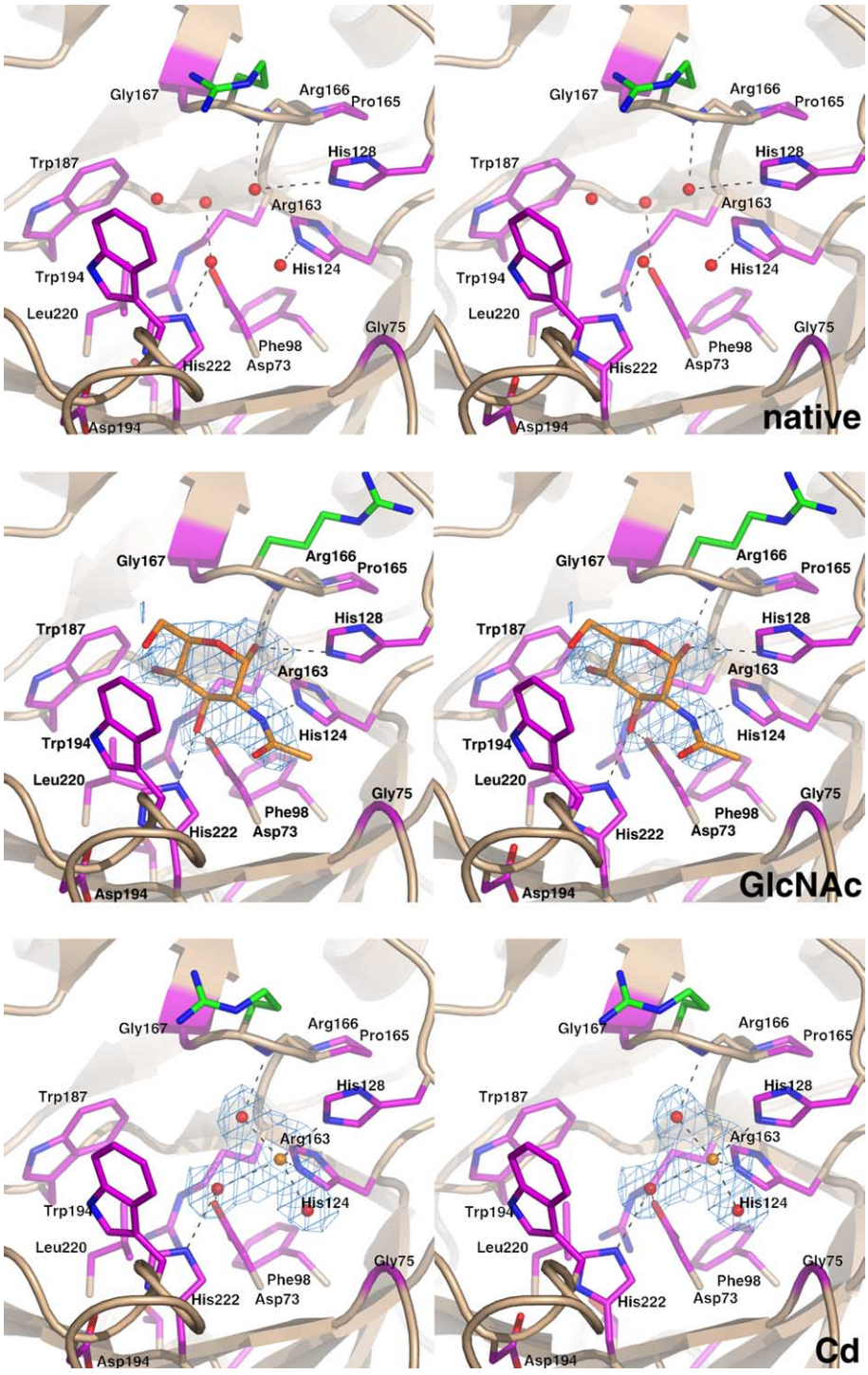

Fig. 3. Details of the active site. The native PdaA structure (“native”), the PdaA–GlcNAc complex (“GlcNAc”) and the PdaA–cadmium (“Cd”) complex are shown. The protein is shown as a ribbon, with residues lining the active site shown as sticks. Residues conserved across the CE-4 family (see also Fig. 1B) are shown with magenta carbons. Arg166, which is unique to PdaA, is shown with green carbons. Key water molecules are shown as red spheres. Hydrogen bonds are shown as black dashed lines. Unbiased (i.e. before including the ligands in the refinement) $|F_o| - |F_c|$, ϕ_{calc} maps are shown in blue, contoured at 2.5σ.

and the other conserved nearby histidines (His124 and His128) also yielded no significant hits. It is possible that this unique arrangement of active site residues in PdaA and other NodB domain proteins plays a key role in an as yet unexplored enzymatic reaction mechanism.

3.3. Complexes with cadmium and N-acetyl-glucosamine

Several studies report that the activity of the yeast chitin deacetylase is cobalt-dependent [1,10,24]. The native enzyme is heavily glycosylated; deglycosylation leads to loss of activity which can be rescued by addition of $CoCl_2$ [10]. Surprisingly,

however, such divalent cation-dependent activity has not been reported for other CE-4 enzymes, such as rhizobial NodB [6], other chitin deacetylases [4,9,11] and peptidoglycan deacetylases, including PdaA [7,8]. We have soaked our crystals with $ZnCl_2$, yet have not observed any density compatible with a zinc ion in the active site. However, when $CdCl_2$ was used as an additive in the mother liquor, it improved the size of the crystals and provided a suitable derivative for experimental phasing, but only after additional soaking at 33 mM concentrations. Inspection of a difference electron density map revealed strong (21σ) positive density in the active site, which refined well as a Cd^{2+} ion (Table 1, Fig. 3). The structure suggests hexagonal coordination in the shape of a tetragonal bipyramid, although one of the axial ligands is missing. The ion coordinates only two of the active site residues, the conserved His124 and His128, the remaining ligands are water molecules (Fig. 3). It is not clear whether the Cd^{2+} complex has any physiological relevance. Although the structure shows coordination with two conserved histidines, further Cd^{2+} sites were observed, formed by solvent exposed histidines elsewhere on the structure. Further experiments will be needed to establish if CE-4 esterases are metalloenzymes. Although many other carbohydrate deacetylases have been shown to be metal-dependent and indeed crystallised as complexes with relevant divalent cations (e.g. [26–28]), there are also examples of metal-independent enzymes (e.g. [29,30]).

Although total synthesis of a peptidoglycan dimer (GlcNAc–MurNAc) has recently been described [31], the pure tetramer, which PdaA requires for activity [8,12], is not available in the quantities and purity required for crystallographic and enzymological studies. We have tried to approach a PdaA–substrate complex by soaking studies with short chitooligosaccharides and the monomers GlcNAc, GlcN, MurNAc and Mur. Using this approach, a PdaA–GlcNAc complex was obtained and refined to 2.25 Å resolution (Fig. 3, Table 1). The unbiased difference electron density map shows the sugar to be in the α-configuration. Binding of GlcNAc displaces several ordered water molecules from the active site, without inducing a significant conformational change (Cα RMSD with native structure is 0.3 Å). The GlcNAc O1, N2, O3 and O4 atoms all occupy positions to within 0.3–0.9 Å from the positions of equivalent water molecules in the native PdaA structure (Fig. 3). All three conserved histidines in the active site interact with the ligand. His124 accepts a hydrogen bond from N2, His128 hydrogen bonds with O1 and His222 hydrogen bonds with O3. In addition, the conserved Asp73 accepts a hydrogen bond from O3. Thus, the GlcNAc sugar only interacts with residues that are fully conserved in family 4 carbohydrate esterases (Figs. 1B and 3), and we propose that this defines the "0" subsite, following the recently proposed subsite nomenclature for this family [11]. Arg166, which is unique to PdaA, could perhaps serve to stabilise or select for the muramic *O*-lactoyl group. Although the PdaA–GlcNAc complex does not reveal the details of the reaction mechanism, is seems possible that His124 is involved in the first step of the reaction. However, it is not yet clear how the same active site His124 could act on both *N* and *O*-acetylated carbohydrate substrate as this would involve either accepting (in case of *N*-acetylated substrate) or donating (in case of *O*-acetylated substrate) a hydrogen bond. Furthermore, unlike GlcNAc, MurNAc carries an *O*-lactoyl group on the 3 position for which there appears to be little room as the GlcNAc 3-OH is pointing down towards the bottom of the groove rather than up towards the solvent (Fig. 3). It is thus possible that this represents a non-productive binding mode, while still giving insights into how this class of enzymes could interact with carbohydrate substrates. Mutagenesis studies and complexes with oligosaccharides will be needed for CE-4 esterases to understand the details of their reaction mechanism. The PdaA structures described here provide a framework for such experiments.

Acknowledgements: We thank the European Synchrotron Radiation Facility, Grenoble, and EMBL/DESY for the time at beamline ID29 and X11, respectively. DvA is supported by a Wellcome Trust Senior Research Fellowship and by the EMBO Young Investigator Programme. We thank Alex Schuettelkopf for fruitful discussions. The coordinates and structure factors have been deposited with the PDB for immediate release on publication (entries 1W17, 1W1A, 1W1B).

References

[1] Caufrier, F., Martinou, A., Dupont, C. and Bouriotis, V. (2003) Carbohydrate esterase family 4 enzymes: substrate specificity. Carbohydr. Res. 338, 687–692.
[2] Kafetzopoulos, D., Thireos, G., Vournakis, J.N. and Bouriotis, V. (1993) The primary structure of a fungal chitin deacetylase reveals the function for 2 bacterial gene-products. Proc. Natl. Acad. Sci. USA 90, 8005–8008.
[3] Mishra, C., Semino, C.E., McCreath, K.J., DelaVega, H., Jones, B.J., Specht, C.A. and Robbins, P.W. (1997) Cloning and expression of two chitin deacetylase genes of *Saccharomyces cerevisiae*. Yeast 13, 327–336.
[4] Tokuyasu, K., Mitsutomi, M., Yamaguchi, I., Hayashi, K. and Mori, Y. (2000) Recognition of chitooligosaccharides and their *n*-acetyl groups by putative subsites of chitin deacetylase from a deuteromycete, *Colletotrichum lindemuthianum*. Biochemistry 39, 8837–8843.
[5] Long, S.R. (1989) Rhizobium-legume nodulation – life together in the underground. Cell 56, 203–214.
[6] John, M., Rohrig, H., Schmidt, J., Wieneke, U. and Schell, J. (1993) Rhizobium NodB protein involved in nodulation signal synthesis is a chitooligosaccharide deacetylase. Proc. Natl. Acad. Sci. USA 90, 625–629.
[7] Vollmer, W. and Tomasz, A. (2000) The pgda gene encodes for a peptidoglycan *n*-acetylglucosamine deacetylase in *Streptococcus pneumoniae*. J. Biol. Chem. 275, 20496–20501.
[8] Fukushima, T., Yamamoto, H., Atrih, A., Foster, S.J. and Sekiguchi, J. (2002) A polysaccharide deacetylase gene (pdaa) is required for germination and for production of muramic delta-lactam residues in the spore cortex of *Bacillus subtilis*. J. Bacteriol. 184, 6007–6015.
[9] Tsigos, I., Zydowicz, N., Martinou, A., Domard, A. and Bouriotis, V. (1999) Mode of action of chitin deacetylase from *Mucor rouxii* on nacetylchitooligosaccharides. Eur. J. Biochem. 261, 698–705.
[10] Martinou, A., Koutsioulis, D. and Bouriotis, V. (2002) Expression, purification, and characterization of a cobaltactivated chitin deacetylase (cda2p) from *Saccharomyces cerevisiae*. Protein Expr. Purif. 24, 111–116.
[11] Hekmat, O., Tokuyasu, K. and Withers, S.G. (2003) Subsite structure of the endo-type chitin deacetylase from a deuteromycete, *Colletotrichum lindemuthianum*: an investigation using steady-state kinetic analysis and ms. Biochem. J. 374, 369–380.
[12] Gilmore, M.E., Dandyopadhyay, D., Dean, A.M., Linnstaedt, S.D. and Popham, D.L. (2004) Production of muramic beta-lactam in *Bacillus subtilis* spore peptidoglycan. J. Bacteriol. 186, 80–89.
[13] Warth, A.D. and Strominger, J.L. (1972) Structure of the peptidoglycan from spores of *Bacillus subtilis*. Biochemistry 11, 1389–1396.
[14] Popham, D.L., Helin, J., Costello, C.E. and Setlow, P. (1996) Muramic lactam in peptidoglycan of *Bacillus subtilis* spores is required for spore outgrowth but not for spore dehydration or heat resistance. Proc. Natl. Acad. Sci. USA 93, 15405–15410.

[15] Otwinowski Z. Daresbury study weekend proceedings.
[16] Lu, G. (1999) Findncs: a program to detect non-crystallographic symmetries in protein crystals from heavy atoms sites. J. Appl. Crystallogr. 32, 365–368.
[17] Cowtan, K. (1994) Joint CCP4 and ESF-EACBM Newsletter on Protein Crystallography, vol. 31, pp. 34–38.
[18] Terwilliger, T.C. (2003) Solve and resolve: automated structure solution and density modification. Methods Enzymol. 374, 22–37.
[19] Perrakis, A., Morris, R. and Lamzin, V.S. (1999) Automated protein model building combined with iterative structure refinement. Nature Struct. Biol. 6, 458–463.
[20] Jones, T.A., Zou, J.Y., Cowan, S.W. and Kjeldgaard, M. (1991) Improved methods for building protein models in electron density maps and the location of errors in these models. Acta Crystallogr. A 47, 110–119.
[21] Brunger, A.T., Adams, P.D., Clore, G.M., Gros, P., Grosse-Kunstleve, R.W., Jiang, J.-S., Kuszewski, J., Nilges, M., Pannu, N.S., Read, R.J., Rice, L.M., Simonson, T. and Warren, G.L. (1998) Crystallography and NMR system: a new software system for macromolecular structure determination. Acta Crystallogr. D 54, 905–921.
[22] Holm, L. and Sander, C. (1993) Protein structure comparison by alignment of distance matrices. J. Mol. Biol. 233, 123–138.
[23] Walden, H., Bell, G.S., Russell, R.J.M., Siebers, B., Hensel, R. and Taylor, G.L. (2001) Tiny tim: a small, tetrameric, hyperthermostable triosephosphate isomerase. J. Mol. Biol. 306, 745–757.
[24] Martinou, A., Koutsioulis, D. and Bouriotis, V. (2003) Cloning and expression of a chitin deacetylase gene (cda2) from *Saccharomyces cerevisiae* in *Escherichia coli* – purification and characterization of the cobalt-dependent recombinant enzyme. Enzyme Microb. Technol. 32, 757–763.
[25] Madsen, D. and Kleywegt, G.J. (2002) Interactive motif and fold recognition in protein structures. J. Appl. Crystallogr. 35, 137–139.
[26] Whittington, D.A., Rusche, K.M., Shin, H., Fierke, C.A. and Christianson, D.W. (2003) Crystal structure of lpxc, a zinc-dependent deacetylase required for lipid a biosynthesis. Abstr. Pap. Am. Chem. Soc. 226, 001-BIOL.
[27] Vincent, F., Yates, D., Garman, E., Davies, G.J. and Brannigan, J.A. (2004) The three-dimensional structure of the *n*-acetylglucosamine-6-phosphate deacetylase, naga, from *Bacillus subtilis* – a member of the urease superfamily. J. Biol. Chem. 279, 2809–2816.
[28] McCarthy, A.A., Peterson, N.A., Knijff, R. and Baker, E.N. (2004) Crystal structure of mshb from *Mycobacterium tuberculosis*, a deacetylase involved in mycothiol biosynthesis. J. Mol. Biol. 335, 1131–1141.
[29] Chang, J.H., Kim, H.C., Hwang, K.Y., Lee, J.W., Jackson, S.P., Bell, S.D. and Cho, Y. (2002) Structural basis for the nad-dependent deacetylase mechanism of sir2. J. Biol. Chem. 277, 34489–34498.
[30] Vincent, F., Charnock, S.J., Verschueren, K.H.G., Turkenburg, J.P., Scott, D.J., Offen, W.A., Roberts, S., Pell, G., Gilbert, H.J., Davies, G.J. and Brannigan, J.A. (2003) Multifunctional xylooligosaccharide/cephalosporin c deacetylase revealed by the hexameric structure of the *Bacillus subtilis* enzyme at 1.9 angstrom resolution. J. Mol. Biol. 330, 593–606.
[31] Keglevic, D., Kojic-Prodic, B. and Tomisic, Z.B. (2003) Synthesis and conformational analysis of the repeating units of bacterial spore peptidoglycan. Carbohydr. Res. 338, 1299–1308.
[32] Bond, C.S. (2003) Topdraw: a sketchpad for protein structure topology cartoons. Bioinformatics 19, 311–312.
[33] Nicholls, A., Sharp, K. and Honig, B. (1991) Protein folding and association – insights from the interfacial and thermodynamic properties of hydrocarbons. Proteins 11, 281–296.